Article

Passive Reactive Power Compensators for Improving the Sustainability of Three-Phase, Four-Wire Sinusoidal Systems Supplied by Unbalanced Voltages

Elisa Peñalvo-López *, Vicente León-Martínez, Joaquín Montañana-Romeu and Javier Cárcel-Carrasco

Institute for Energy Engineering, Universitat Politècnica de València, 46022 Valencia, Spain; vleon@die.upv.es (V.L.-M.); jmontanana@die.upv.es (J.M.-R.); fracarc1@csa.upv.es (J.C.-C.)

* Correspondence: elpealpe@upvnet.upv.es; Tel.: +34-96-387-59-35

Abstract: Compensation of reactive power is necessary in power systems due to economical, energetic, and environmental reasons. Reactive power increases energy power losses and carbon dioxide emissions in distribution lines and power transformers. However, capacitor banks used in most industrial applications do not significantly reduce energy losses in lines and transformers when supply voltages and loads are unbalanced and therefore do not fully improve the sustainability of distribution networks. This fact is explained in this paper using positive-, negative-, and zero-sequence reactive power components in three-phase, four-wire sinusoidal power systems supplied with unbalanced voltages. Likewise, several devices have also been developed for the compensation of the total reactive power and, specifically, for each of its components in these power systems. Comparing the effectiveness of these reactive compensators and other well-known passive compensators as capacitor banks on the sustainability improvement of the electrical installation of an actual industry, reductions between 20% and 100% in energy losses and carbon dioxide emissions, caused by circulation of reactive currents in transformer and lines, can be expected depending on the type of compensator used.

Keywords: reactive power; reactive components; reactive compensation; unbalanced systems; sustainability

1. Introduction

Reactive power has been a well-known quantity in the technical literature since Stanley [1], Schallenberger [2], and Steinmetz [3] physically and mathematically explained this phenomenon in single-phase sinusoidal systems in the late 19th century. The formulation and physical meaning of reactive power have been extensively studied throughout the 20th century [4–7], and even today [8,9]. The IEEE Standard 1459 [10] defines the reactive power as the fundamental frequency.

Likewise, this standard defines three reactive power components in three-phase, four-wire systems based on Fortescue's contributions [11,12]. These reactive power components are the positive-, negative- and zero-sequence reactive powers in three-phase, four-wire systems. The scientific community has accepted the physical meanings of these reactive power components, which are actually included in the IEEE Standard 1459. The positive-sequence reactive power (Q_+) is the most important reactive power component in power systems, much more than the zero-sequence reactive power (Q_0). The negative-sequence reactive power (Q_-) is usually negligible because of the limitations of the zero-sequence voltages below 1–2% imposed by the standards [13–18].

The interest in positive-sequence reactive powers is because these reactive power components determine the correct operation and stability of generators and motors in

power systems, as the IEEE Standard 1459 establishes in its introduction. However, nowadays there are no passive devices for compensating Q_+ separately from Q_- and Q_0. There are also no devices able to maintain the values of Q_+ while the other two reactive power components' resulting voltage imbalances (Q_- and Q_0) are cancelled. All compensation devices, passive and active, today known in the technical literature are used to compensate the total reactive power, i.e., they can cancel the three reactive power components (Q_+, Q_-, and Q_0) at once, but these devices are not able to compensate for the reactive power components separately.

This is the case with capacitor banks used in most industrial applications. These passive devices minimize the total reactive power supplied by the sources, but they are not able to reduce significantly the reactive currents when supply voltages and loads are unbalanced, such as it will be noted in the application example and was theoretically demonstrated in [19]. Since 2010, several passive reactive power compensators have been developed to operate in unbalanced voltage conditions [20–22]. These devices compensate for the total reactive power in three-phase, four-wire power systems, while they also balance the active currents. Active devices for reactive power compensation are also well known in the technical literature, such as SVCs and STATCOMs [23–38]. The former is fundamentally dedicated to reactive power compensation, while the latter can also be applied to unbalanced compensation and, above all, harmonic filtering. These active devices are not the object of study in this paper, which is focused on passive reactive power compensators.

Due to the fact there are no passive devices in the technical literature for separately compensating each reactive power component (Q_+, Q_-, and Q_0), the development of these passive compensators for three-phase, four-wire sinusoidal systems is the main novelty of this paper. Specifically, the following devices are theoretically developed in Section 3 for three-phase, four-wire sinusoidal systems supplied by unbalanced voltages:

- Individual compensators for the positive-sequence reactive powers (Figure 1a), which minimize or cancel the supply of Q_+ without affecting the values of the other reactive power components (Q_- and Q_0).
- Combined compensators for the negative- and zero-sequence reactive powers (Figure 1b), which remove the supply of negative- and zero-sequence reactive powers (Q_-, Q_0) keeping invariable the values of positive-sequence reactive powers (Q_+).
- Individual compensators for the negative-sequence (Figure 1c) and the zero-sequence (Figure 1d) reactive powers, which respectively cancel Q_- and Q_0. The first individual devices do not modify the values of Q_+ and Q_0, whereas the second individual compensators do not affect the values of Q_+ and Q_-.
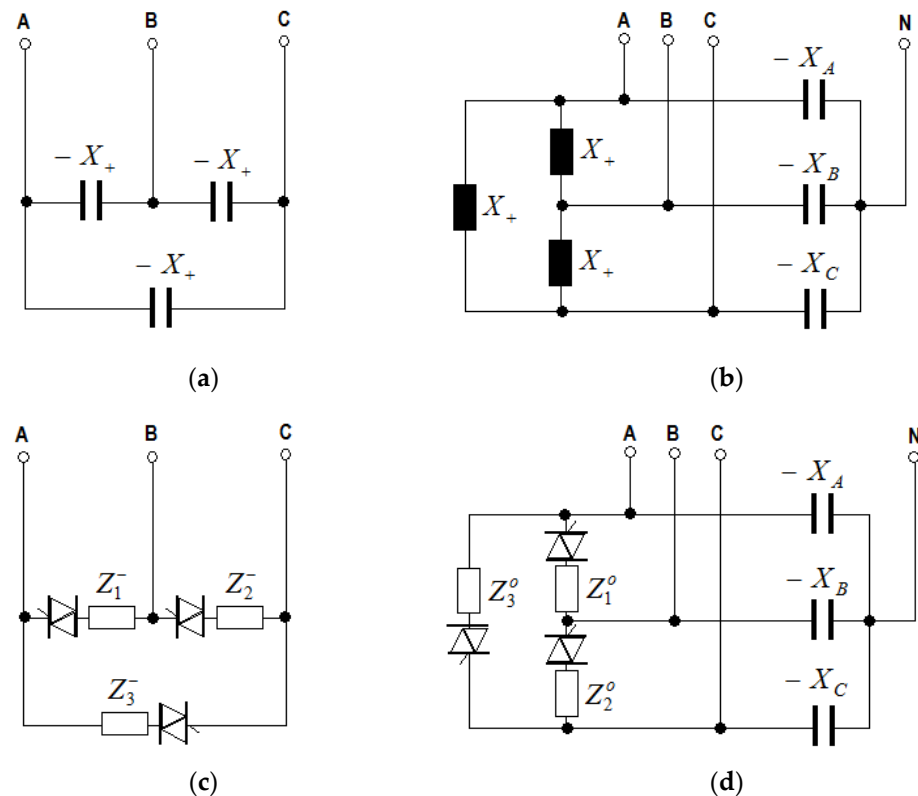
Figure 1. Compensators for reactive power components: (**a**) individual positive-sequence reactive compensators; (**b**) combined compensators of negative- and zero-sequence reactive powers; (**c**) a possible implementation of individual negative-sequence reactive compensators; and (**d**) a possible implementation of individual zero-sequence reactive power compensators.

The individual compensators of positive-sequence reactive powers and the combined compensators are theoretically developed in Sections 3.2. and 3.3.1., respectively. These devices are formed by passive reactances (coils and capacitors), as Figures 1a and 1b represent, and they have important practical applications either minimizing the positive-sequence currents or removing the reactive currents caused by imbalances, respectively. These current reductions are useful to improve the sustainability of electrical networks by reducing power losses in transformers and lines.

Conversely, the individual compensators of negative- and zero-sequence reactive powers are less effective in reducing the reactive currents than the combined compensators listed above. Likewise, the phase impedances of these individual compensators have angles greater than ±90° and, thus, they are active devices because they must be formed by electronic converters (Figures 1c and 1d) and, therefore, are more expensive than the combined compensators of Figure 1b. These reasons justify the individual compensators of negative- and zero-sequence reactive powers being out of the title of this paper, which is focused in passive compensators. However, these active devices are theoretically developed in Section 3.3.2. as an additional contribution of this paper and they are not practically implemented.

Topology and elements of all reactive power compensators mentioned above have been determined by applying Ohm's law and Fortescue's theorem [11] under the consideration these devices must supply fundamental-frequency reactive currents of positive, negative and zero sequences. The use of Fortescue's theorem is the key that determines topology differences between our compensators and the industrial capacitor banks, Jeon's compensators, and similar passive devices described in [21,22]. Since Fortescue's theorem is not applied to implement latter passive compensators, these can only compensate the

total reactive powers, but they are not able to compensate separately each of the reactive power components.

Finally, in Section 4, the operation of the reactive power passive compensators developed in this paper is tested in an application example on the actual unbalanced electrical installation of a manufacturer of frozen products. Likewise, the effectiveness of these passive devices on the sustainability improvement in the transformer and lines of that installation are been compared with those obtained from the capacitor banks and Jeon's compensators [20]. The comparison determines that:

- The individual compensators for the positive-sequence reactive powers reduce energy source losses and carbon dioxide emissions caused by circulation of reactive currents in a similar amount as the traditional capacitor banks (60–80%).
- The combined compensators of negative- and zero-sequence reactive powers cancel energy losses occurred in the neutral conductor, but they achieve modest reductions in source energy losses and carbon dioxide emissions due to circulation of reactive currents (20–40%).
- The total reactive power compensators (TRPC) reduce 100% of energy source losses and carbon dioxide emissions caused by circulation of reactive currents, which is not possible with the capacitor banks today used in industrial applications.

2. Active and Reactive Power Components in Unbalanced Systems

In this section, the expressions for the positive-, negative-, and zero-sequence components of the active and reactive powers are established for the three-phase, four-wire sinusoidal and unbalanced system represented in Figure 2 using Ohm's and Kirchhoff's laws and Fortescue's theorem.
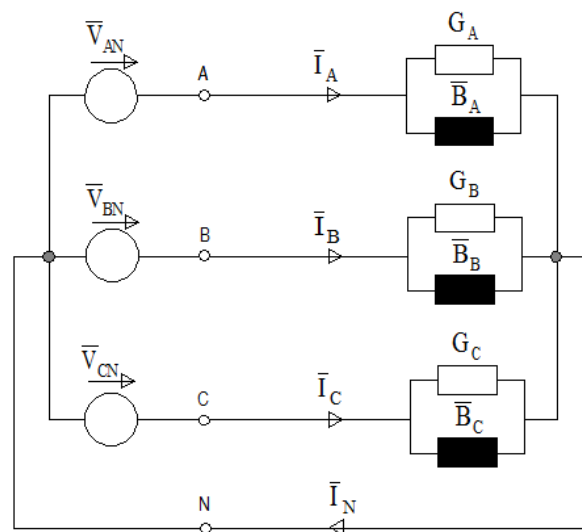
Figure 2. Three-phase, four-wire sinusoidal system.

Considering that both the source and the load of the three-phase sinusoidal system in Figure 2 are unbalanced, in general, and these subsystems are connected through lines and neutral wires of negligible impedances, the Complex Root Mean Square (CRMS) line ($\bar{I}_z$) and neutral ($\bar{I}_N$) currents ($z = A, B, C$) of this system are, according to Ohm's and the first of Kirchhoff's laws, as follows,

$$\bar{I}_z = \bar{Y}_z \cdot \bar{V}_{zN} = (G_z + \bar{B}_z) \cdot \bar{V}_{zN} = \bar{I}_{za} + \bar{I}_{zr}$$

$$\bar{I}_N = \sum_{z=A,B,C} (G_z + \bar{B}_z) \cdot \bar{V}_{zN} \qquad (1)$$

$\bar{V}_{zN}$ being the line-to-neutral voltages, $\bar{Y}_z = G_z + \bar{B}_z$ the load complex admittances, expressed as a function of the load conductances (G_z) and susceptances $(\bar{B}_z)$, and $\bar{I}_{za} = G_z \cdot \bar{V}_{zN}$ and $\bar{I}_{zr} = \bar{B}_z \cdot \bar{V}_{zN}$ are the active and reactive line currents of each phase $(z = A, B, C)$, respectively.

Since voltages and currents of the system in Figure 2 are generally unbalanced, these quantities can be decomposed into their positive- (+), negative- (−), and zero-sequence (0) components, according to Fortescue's theorem [11]. Thus, if the symmetrical components of the line-to-neutral voltages are $\bar{V}_{AN+} = V_+ \angle \alpha_+, \bar{V}_{AN-} = V_- \angle \alpha_-, \bar{V}_{AN0} = V_0 \angle \alpha_0$, the line currents can be decomposed as follows:

$$\bar{I}_{A+} = \frac{1}{3}(\bar{I}_A + a\,\bar{I}_B + a^2\bar{I}_C) = (\bar{Y}_{b+} + \bar{\delta}_U\bar{Y}_i + \bar{\delta}_0\bar{Y}_h) \cdot \bar{V}_{AN+} = \bar{Y}_+ \cdot \bar{V}_{AN+}$$

$$\bar{I}_{A-} = \frac{1}{3}(\bar{I}_A + a^2\bar{I}_B + a\,\bar{I}_C) = \frac{1}{\bar{\delta}_U}(\bar{Y}_h + \bar{\delta}_U\bar{Y}_{b-} + \bar{\delta}_0\bar{Y}_i) \cdot \bar{V}_{AN-} = \bar{Y}_- \cdot \bar{V}_{AN-}$$

$$\bar{I}_{A0} = \frac{1}{3}(\bar{I}_A + \bar{I}_B + \bar{I}_C) = \frac{1}{\bar{\delta}_0}(\bar{Y}_i + \bar{\delta}_U\bar{Y}_{b-} + \bar{\delta}_0\bar{Y}_h) \cdot \bar{V}_{AN0} = \bar{Y}_0 \cdot \bar{V}_{AN0} \tag{2}$$

where $a = e^{j120°}$,

$$\bar{\delta}_U = \frac{\bar{V}_{AN-}}{\bar{V}_{AN+}} = \delta_U \angle(\alpha_- - \alpha_+) \qquad \bar{\delta}_0 = \frac{\bar{V}_{AN0}}{\bar{V}_{AN+}} = \delta_0 \angle(\alpha_0 - \alpha_+) \tag{3}$$

are the negative-sequence unbalance factor $(\bar{\delta}_U)$ and the zero-sequence unbalance factor $(\bar{\delta}_0)$ of the line-to-neutral voltages,

$$\bar{Y}_+ = \frac{\bar{I}_{A+}}{\bar{V}_{AN+}} = G_+ + \bar{B}_+ \qquad \bar{Y}_- = \frac{\bar{I}_{A-}}{\bar{V}_{AN-}} = G_- + \bar{B}_- \qquad \bar{Y}_0 = \frac{\bar{I}_{A0}}{\bar{V}_{AN0}} = G_0 + \bar{B}_0 \tag{4}$$

are the complex admittances for the positive-, negative-, and zero-sequences, expressed as a function of the respective conductances (G_+, G_-, G_0) and complex susceptances $(\bar{B}_+, \bar{B}_-, \bar{B}_0)$,

$$\bar{Y}_{b+} = \frac{1}{3}(\bar{Y}_A + \bar{Y}_B + \bar{Y}_C) = Y_{b+} \angle -\varphi_{b+} = G_{b+} + \bar{B}_{b+} \tag{5}$$

are the well-known complex admittance of the load supplied with positive-sequence voltages, and

$$\bar{Y}_i = \frac{\bar{I}_{A+}}{\bar{V}_{AN-}} = \frac{\bar{I}_{A-}}{\bar{V}_{AN0}} = \frac{\bar{I}_{A0}}{\bar{V}_{AN+}} = \frac{1}{3}(\bar{Y}_A + a^2\bar{Y}_B + a\,\bar{Y}_C) = Y_i \angle -\varphi_i$$

$$\tag{6}$$

$$\bar{Y}_h = \frac{\bar{I}_{A+}}{\bar{V}_{AN0}} = \frac{\bar{I}_{A-}}{\bar{V}_{AN+}} = \frac{\bar{I}_{A0}}{\bar{V}_{AN-}} = \frac{1}{3}(\bar{Y}_A + a\,\bar{Y}_B + a^2\bar{Y}_C) = Y_h \angle -\varphi_h$$

are the ratios between voltages and currents of different sequences, which have dimensions of admittance and are defined in systems with both asymmetrical sources and loads.

The complex power supplied by the source and absorbed by the load of the system represented in Figure 1 can be determined as a function of the line-to-neutral voltages and line currents,

$$\bar{S} = \bar{V}_{AN} \cdot \bar{I}_A^* + \bar{V}_{BN} \cdot \bar{I}_B^* + \bar{V}_{CN} \cdot \bar{I}_C^* = P + \bar{Q} \tag{7}$$

where P and $\bar{Q}$ are the active and complex reactive powers, respectively,

$$P = G_A \cdot V_{AN}^2 + G_B \cdot V_{BN}^2 + G_C \cdot V_{CN}^2 \qquad \bar{Q} = \bar{B}_A^* \cdot V_{AN}^2 + \bar{B}_B^* \cdot V_{BN}^2 + \bar{B}_C^* \cdot V_{CN}^2 \tag{8}$$

and the asterisk (*) denotes the conjugate of a complex quantity. The complex power can also be expressed as a function of the complex powers corresponding to each sequence as follows [10]:

$$\bar{S} = \bar{S}_+ + \bar{S}_- + \bar{S}_0 = 3\,\bar{V}_{AN+}\bar{I}_{A+}^* + 3\,\bar{V}_{AN-}\bar{I}_{A-}^* + 3\,\bar{V}_{AN0}\bar{I}_{A0}^* = P + \bar{Q} \tag{9}$$

The real part of the complex power $(\bar{S})$ is the active power (P) and the imaginary part is the reactive power $(\bar{Q})$,

$$P = P_+ + P_- + P_0 \qquad \bar{Q} = \bar{Q}_+ + \bar{Q}_- + \bar{Q}_0 \tag{10}$$

where (P_+, P_-, P_0) and $(\bar{Q}_+, \bar{Q}_-, \bar{Q}_0)$ are the well-known active and complex reactive powers, respectively defined in [10] for the positive-, negative-, and zero-sequence voltages and currents.

2.1. Positive-Sequence Active and Reactive Powers

Positive-sequence active and reactive powers $(P_+, \bar{Q}_+)$ are the main components of the complex power supplied by the generators in power plants and transferred through the high voltage (HV) lines as well as delivered in most low voltage (LV) distribution networks.

According to the first Equation (2), the positive-sequence complex apparent power can be expressed as follows:

$$\bar{S}_+ = 3\,\bar{V}_{AN+} \cdot \bar{I}_{A+}^* = 3\,\bar{Y}_+^* \cdot V_{AN+}^2 = P_+ + \bar{Q}_+ \tag{11}$$

where the conjugate of the positive-sequence admittance of the load is

$$\bar{Y}_+^* = \bar{Y}_{b+}^* + \bar{\delta}_U^* \bar{Y}_i^* + \bar{\delta}_0^* \bar{Y}_h^* = G_+ + \bar{B}_+^* \tag{12}$$

The real part of $\bar{S}_+$ is the positive-sequence active power (P_+),

$$P_+ = 3\,G_+ V_{AN+}^2 \tag{13}$$

The imaginary part of $\bar{S}_+$ is the positive-sequence reactive power $(\bar{Q}_+)$,

$$\bar{Q}_+ = 3\,\bar{B}_+^* V_{AN+}^2 \tag{14}$$

2.2. Negative- and Zero-Sequence Active and Reactive Powers

The negative- and zero-sequence active and reactive powers usually occur because of the voltage imbalances in power systems.

The negative-sequence complex power is expressed as follows:

$$\bar{S}_- = 3\,\bar{V}_{AN-} \cdot \bar{I}_{A-}^* = 3\,\bar{Y}_-^* V_{AN-}^2 = P_- + \bar{Q}_- \tag{15}$$

in which

$$P_- = 3\,G_- V_{AN-}^2 \qquad \bar{Q}_- = 3\,\bar{B}_-^* V_{AN-}^2 \tag{16}$$

are the negative-sequence active and reactive powers, respectively, and the negative conductance (G_-) and susceptance $(\bar{B}_-)$ are defined by the second Equation (4). The negative-sequence active and reactive powers are responsible of malfunctions in the operation of three-phase generators and motors [13,14,16]. Therefore, the negative-sequence unbalanced voltage factors are limited to values less than 1–2% by several standards [13–18] in order to reduce the negative-sequence powers.

The zero-sequence complex power has the following expression:

$$\bar{S}_0 = 3\,\bar{V}_{AN0} \cdot \bar{I}_{A0}^* = 3\,\bar{Y}_0^* V_{AN0}^2 = P_0 + \bar{Q}_0 \tag{17}$$

where

$$P_0 = 3\,G_0 \cdot V_{AN0}^2 \qquad \bar{Q}_0 = 3\,\bar{B}_0^* \cdot V_{AN0}^2 \tag{18}$$

are the zero-sequence active and reactive powers, respectively, which occur because of either source malfunctions or displacement of the source and load neutral points, and the zero conductance (G_0) and susceptance $(\bar{B}_0)$ are determined by the third Equation (4).

3. Devices for the Compensation of Reactive Powers

The reactive power compensators that can supply the total reactive power $(\bar{Q})$ absorbed by the load in Figure 2, as well as those that separately compensate the positive- $(\bar{Q}_+)$, negative- $(\bar{Q}_-)$, and zero-sequence $(\bar{Q}_0)$ reactive powers, are described in this section. These devices are formed, in general, by two three-phase configurations: one in delta, with admittances $(\bar{Y}_{AB}^c, \bar{Y}_{BC}^c,$ and $\bar{Y}_{CA}^c)$, and the other star-configured, with admittances $(\bar{Y}_A^c, \bar{Y}_B^c,$ and $\bar{Y}_C^c)$, which is equipped with a neutral conductor (Figure 3).
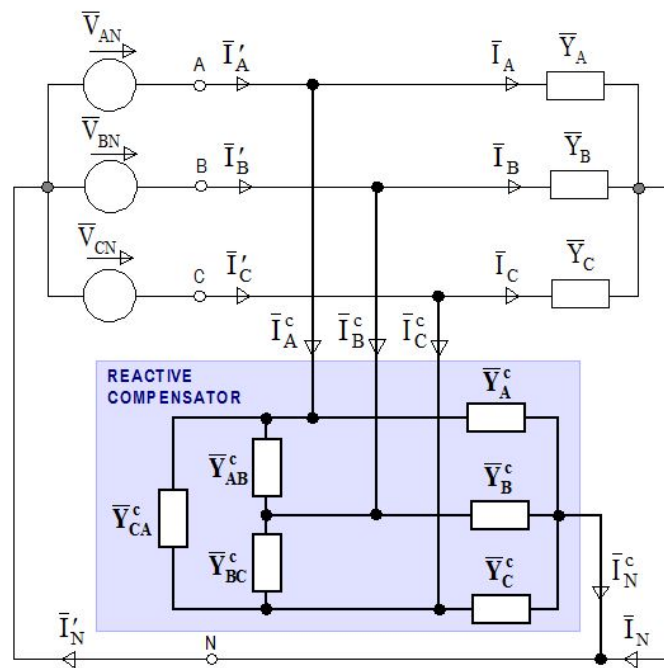
Figure 3. General constitution and placement of the reactive power compensators in three-phase, four-wire power systems.

3.1. Total Reactive Power Compensators (TRPC)

These compensation devices must deliver the reactive powers ($\bar{Q}_z = \bar{B}_z^* \cdot V_{zN}^2$) and currents ($\bar{I}_{zr} = \bar{B}_z \cdot \bar{V}_{zN}$) absorbed in each phase ($z = A, B, C$) by the load in Figure 2. Therefore, the currents absorbed by the reactive compensator have to be opposite to the load reactive currents, as follows:

$$
\begin{aligned}
\bar{I}_A^c &= \bar{Y}_A^c \cdot \bar{V}_{AN} + \bar{Y}_{AB}^c \bar{V}_{AB} - \bar{Y}_{CA}^c \bar{V}_{CA} = -\bar{I}_{Ar} = -\bar{B}_A \cdot \bar{V}_{AN} \\
\bar{I}_B^c &= \bar{Y}_B^c \cdot \bar{V}_{BN} + \bar{Y}_{BC}^c \bar{V}_{BC} - \bar{Y}_{AB}^c \bar{V}_{AB} = -\bar{I}_{Br} = -\bar{B}_B \cdot \bar{V}_{BN} \\
\bar{I}_C^c &= \bar{Y}_C^c \cdot \bar{V}_{CN} + \bar{Y}_{CA}^c \bar{V}_{CA} - \bar{Y}_{BC}^c \bar{V}_{BC} = -\bar{I}_{Cr} = -\bar{B}_C \cdot \bar{V}_{CN}
\end{aligned}
\tag{19}
$$

Solutions for the above equations determine that the admittances ($\bar{Y}_{AB}^c, \bar{Y}_{BC}^c, \bar{Y}_{CA}^c$) and ($\bar{Y}_A^c, \bar{Y}_B^c, \bar{Y}_C^c$) of the total reactive compensator must have the values indicated in Table 1.

Table 1. Admittances of the total reactive power compensator (TRPC).

DELTA CONFIGURATION			STAR CONFIGURATION		
$\bar{Y}_{AB}^c$	$\bar{Y}_{BC}^c$	$\bar{Y}_{CA}^c$	$\bar{Y}_A^c$	$\bar{Y}_B^c$	$\bar{Y}_C^c$
0	0	0	$-\bar{B}_A$	$-\bar{B}_B$	$-\bar{B}_C$

The results summarized in Table 1 are well-known in circuit theory as well as in industrial practice.

The complex power absorbed by this compensator ($\bar{S}_c$) is opposite to the load reactive power, i.e.:

$$
\bar{S}^c = -\bar{Q} = -\bar{B}_A^* \cdot V_{AN}^2 - \bar{B}_B^* \cdot V_{BN}^2 - \bar{B}_C^* \cdot V_{CN}^2,
\tag{20}
$$

Thus, these compensators do not modify the active power (P) delivered by the source, whereas the source reactive power ($\bar{Q}$) is canceled (Table 2).

Table 2. Active and reactive source powers after connecting TRPC ($z = A, B, C$).

ACTIVE POWER	REACTIVE POWER
$\sum_z P_z = \sum_z G_z V_{zN}^2$	$\sum_z (\bar{Q}_z - \bar{Q}_z) = 0$

After connecting the total reactive power compensators, the active currents are not modified, the reactive currents are cancelled, and the neutral current is reduced up to the value:

$$\bar{I}'_N = G_A \bar{V}_{AN} + G_B \bar{V}_{BN} + G_C \bar{V}_{CN} \tag{21}$$

which is three times the zero-sequence component of the active currents absorbed by the load.

3.2. Positive-Sequence Reactive Power Compensators

The reactive powers delivered through the positive-sequence voltages and currents are the main reactive power components in most electrical networks. Thus, compensating the positive-sequence reactive powers ($\bar{Q}_+$) should be of primary interest.

These compensation devices must absorb the positive-sequence reactive powers and currents opposite to those absorbed by the load in unbalanced voltage conditions, namely:

$$\bar{S}^c = -\bar{Q}_+ = -3\,\bar{B}_+^* \cdot V_{AN+}^2 \qquad \bar{I}_z^c = -\bar{I}_{zr+} = -\bar{B}_+ \cdot \bar{V}_{zN+} \quad (z = A, B, C), \tag{22}$$

being $\bar{B}_+$ the positive-sequence load susceptance, determined by Equations (4) and (12).

Therefore, the positive-sequence reactive power compensators do not require a neutral conductor to evacuate the zero-sequence currents and, thus, the star configuration in Figure 3 can be avoided. Hence, these compensation devices are formed by three admittances ($\bar{Y}_{AB}^c, \bar{Y}_{BC}^c, \bar{Y}_{CA}^c$) configured in delta. Further, an additional advantage of this configuration is that the line-to-line voltages are applied to these admittances, which only have positive- and negative-sequence components.

The positive-sequence reactive power compensators are formed by two set of admittances, ($-\frac{1}{3}\bar{B}_+, -\frac{1}{3}\bar{B}_+, -\frac{1}{3}\bar{B}_+$) and ($\bar{Y}_{AB-}^c, \bar{Y}_{BC-}^c, \bar{Y}_{CA-}^c$), which are connected in parallel, as Figure 4 represents.
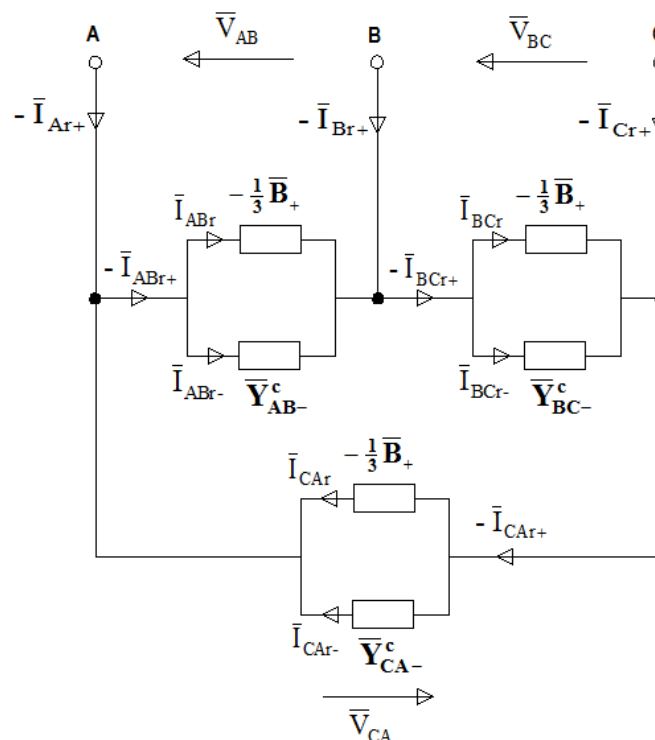
Figure 4. Constitution of the positive-sequence reactive power compensators ($\bar{Q}_+$). (Arrows of the line-to-line voltages indicate the greatest potential point).

The first set of admittances ($-\frac{1}{3}\bar{B}_+, -\frac{1}{3}\bar{B}_+, -\frac{1}{3}\bar{B}_+$) is a three-phase balanced delta configuration that absorbs reactive currents with positive- and negative-sequence components, which are determined according to Ohm's law and Fortescue's theorem:

$$\bar{I}_{ABr} = -\frac{1}{3}\bar{B}_+ \cdot \bar{V}_{AB} = -\frac{1}{3}\bar{B}_+ \cdot (\bar{V}_{AB+} + \bar{V}_{AB-}) = -\bar{I}_{ABr+} - \bar{I}_{ABr-}$$

$$\bar{I}_{BCr} = -\frac{1}{3}\bar{B}_+ \cdot \bar{V}_{BC} = -\frac{1}{3}\bar{B}_+ \cdot (\bar{V}_{BC+} + \bar{V}_{BC-}) = -\bar{I}_{BCr+} - \bar{I}_{BCr-} \qquad (23)$$

$$\bar{I}_{CAr} = -\frac{1}{3}\bar{B}_+ \cdot \bar{V}_{CA} = -\frac{1}{3}\bar{B}_+ \cdot (\bar{V}_{CA+} + \bar{V}_{CA-}) = -\bar{I}_{CAr+} - \bar{I}_{CAr-}$$

This delta-balanced configuration supplies the same positive-sequence reactive powers ($\bar{Q}_+$) absorbed by the load. However, the complex power shows that a negative-sequence reactive power ($\bar{Q}_-$) is additionally engendered due to the negative-sequence line-to-line voltages:

$$-\frac{1}{3}\bar{B}_+^* \cdot (V_{AB}^2 + V_{BC}^2 + V_{CA}^2) = -3\bar{B}_+^* \cdot (V_{AN+}^2 + V_{AN-}^2) = \bar{Q}_+ - \bar{Q}_- \qquad (24)$$

The set of admittances ($-\frac{1}{3}\bar{B}_+, -\frac{1}{3}\bar{B}_+, -\frac{1}{3}\bar{B}_+$) of the $\bar{Q}_+$ compensator are passive reactances (coils and capacitors).

The other set of admittances ($\bar{Y}_{AB-}^c, \bar{Y}_{BC-}^c, \bar{Y}_{CA-}^c$) constitutes a three-phase unbalanced delta configuration (Figure 4) that absorbs the negative-sequence reactive powers ($-\bar{Q}_-$), which are caused by the negative-sequence voltages on the balanced configuration ($-\frac{1}{3}\bar{B}_+, -\frac{1}{3}\bar{B}_+, -\frac{1}{3}\bar{B}_+$) and expressed by Equation (24). For the accomplishment of this goal, the currents flowing through the admittances of this unbalanced configuration are opposite to the negative-sequence currents engendered by the balanced configuration and expressed by (23), namely,

$$\bar{I}_{ABr-} = \frac{1}{3}\bar{B}_+ \cdot \bar{V}_{AB-} \qquad \bar{I}_{BCr-} = \frac{1}{3}\bar{B}_+ \cdot \bar{V}_{BC-} \qquad \bar{I}_{CAr-} = \frac{1}{3}\bar{B}_+ \cdot \bar{V}_{CA-} \qquad (25)$$

Thus, the values of the admittances ($\bar{Y}_{AB-}^c, \bar{Y}_{BC-}^c, \bar{Y}_{CA-}^c$) of this configuration are, according to Ohm's law:

$$\bar{Y}_{AB-}^c = \frac{\bar{I}_{ABr-}}{\bar{V}_{AB}} = \frac{1}{3}\bar{B}_+ \frac{\bar{V}_{AB-}}{\bar{V}_{AB+} + \bar{V}_{AB-}} = -\frac{1}{3}\bar{B}_+ \frac{a\bar{\delta}_U}{1 - a\bar{\delta}_U}$$

$$\bar{Y}_{BC-}^c = \frac{\bar{I}_{BCr-}}{\bar{V}_{BC}} = \frac{1}{3}\bar{B}_+ \frac{a\bar{V}_{AB-}}{a^2\bar{V}_{AB+} + a\bar{V}_{AB-}} = -\frac{1}{3}\bar{B}_+ \frac{\bar{\delta}_U}{1 - \bar{\delta}_U} \qquad (26)$$

$$\bar{Y}_{CA-}^c = \frac{\bar{I}_{CAr-}}{\bar{V}_{CA}} = \frac{1}{3}\bar{B}_+ \frac{a^2\bar{V}_{AB-}}{a\bar{V}_{AB+} + a^2\bar{V}_{AB-}} = -\frac{1}{3}\bar{B}_+ \frac{a^2\bar{\delta}_U}{1 - a^2\bar{\delta}_U}$$

being $\bar{\delta}_U = \bar{V}_{AN-}/\bar{V}_{AN+} = -\bar{V}_{AB-}/a\bar{V}_{AB+}$ the negative-sequence unbalance factor of the line-to-neutral voltages, determined by (3), and $a = e^{j\,120°}$.

The complex power absorbed by these three admittances ($\bar{Y}_{AB-}^c, \bar{Y}_{BC-}^c, \bar{Y}_{CA-}^c$),

$$\bar{V}_{AB} \cdot (\bar{I}_{ABr-}^b)^* + \bar{V}_{BC} \cdot (\bar{I}_{BCr-}^b)^* + \bar{V}_{CA} \cdot (\bar{I}_{CAr-}^b)^* = (1 + a + a^2) \cdot \bar{V}_{AB+} \cdot (\bar{I}_{ABr-}^b)^* +$$
$$+ 3\bar{V}_{AB-} \cdot (\bar{I}_{ABr-}^b)^* = \bar{B}_{b+}^* \cdot V_{AB-}^2 = 3\,\bar{B}_{b+}^* \cdot V_{AN-}^2 = \bar{Q}_{b-} \qquad (27)$$

is opposite to the negative-sequence reactive power in Equation (24).

In summary, the positive-sequence reactive power compensators are formed by three admittances configured in delta ($\bar{Y}_{AB}^c, \bar{Y}_{BC}^c, \bar{Y}_{CA}^c$), determined by the parallel connection (Figure 3) of two sets of admittances, ($-\frac{1}{3}\bar{B}_+, -\frac{1}{3}\bar{B}_+, -\frac{1}{3}\bar{B}_+$) and ($\bar{Y}_{AB-}^c, \bar{Y}_{BC-}^c, \bar{Y}_{CA-}^c$), with no star configuration of admittances ($\bar{Y}_A^c, \bar{Y}_B^c, \bar{Y}_C^c$) in Figure 2, such as Table 3 indicates.

Table 3. Admittances of the positive-sequence reactive power compensators.

DELTA CONFIGURATION			STAR CONFIGURATION		
$\bar{Y}_{AB}^c$	$\bar{Y}_{BC}^c$	$\bar{Y}_{CA}^c$	$\bar{Y}_A^c$	$\bar{Y}_B^c$	$\bar{Y}_C^c$
$-\frac{1}{3}\bar{B}_+ \frac{1}{1-a\bar{\delta}_U}$	$-\frac{1}{3}\bar{B}_+ \frac{1}{1-\bar{\delta}_U}$	$-\frac{1}{3}\bar{B}_+ \frac{1}{1-a^2\bar{\delta}_U}$	0	0	0

According to Equations (24) and (27), the total complex power ($\bar{S}^c$) of these two sets of admittances,

$$\bar{S}^c = -\bar{Q}_+ - \bar{Q}_- + \bar{Q}_- = -\bar{Q}_+ = -3\,\bar{B}_+^* \cdot V_{AN+}^2 \tag{28}$$

is opposite to the positive-sequence reactive power $\bar{Q}_+$ absorbed by the load. Therefore, the compensation devices of positive-sequence reactive power do not affect the values of the active powers delivered by each source phases ($P_z = G_z V_{zN}^2, z = A, B, C$), whereas the source reactive powers are reduced an amount, in each phase ($z = A, B, C$), of value equal to the third part of the reactive power supplied by the compensator ($\bar{Q}_z - \frac{1}{3}\bar{Q}_+$), such as Table 4 summarizes.

Table 4. Active and reactive source powers after connecting the positive-sequence reactive power compensators.

ACTIVE	REACTIVE
$\sum_z P_z = \sum_z G_z V_{zN}^2$	$\sum_z \left(\bar{Q}_z - \frac{1}{3}\bar{Q}_+\right)$

The connection of the positive-sequence reactive power compensators cancels the positive-sequence reactive source currents. The active and neutral currents are not modified, with the same values determined by Equation (1).

Since most standards [13–18] limit the values of the negative-sequence unbalanced voltage factor to values under 1-2% ($\delta_U < 0.02$), the admittances ($\bar{Y}_{AB-}^c, \bar{Y}_{BC-}^c, \bar{Y}_{CA-}^c$) are usually negligible and, therefore, the positive-sequence reactive power compensators can be built, with great approximation, by a balanced delta configuration of susceptances ($-\frac{1}{3}\bar{B}_+, -\frac{1}{3}\bar{B}_+, -\frac{1}{3}\bar{B}_+$).

3.3. Negative- and Zero-Sequence Reactive Power Compensators

Negative- and zero-sequence reactive powers occur because of voltage imbalances and are not usually the main reactive powers in electrical networks. Therefore, these reactive powers should be compensated either by only one combined compensator or by specific compensators of negative- and zero-sequence reactive powers. All these compensation devices are described in this section.

3.3.1. Combined Compensators of Negative- and Zero-Sequence Reactive Powers

These compensators have to supply both the negative- and zero-sequence reactive powers and currents absorbed by the load, namely:

$$\bar{S}^c = -(\bar{Q}_- + \bar{Q}_0) = -\bar{Q} + \bar{Q}_+$$
$$\bar{I}_z^c = -\bar{I}_{zr-} - \bar{I}_{r0} = -\bar{I}_{zr} + \bar{I}_{zr+} \qquad z = (A, B, C), \tag{29}$$

being ($\bar{Q}_-$ and $\bar{Q}_0$) the negative- and zero-sequence reactive powers determined by Equations (28) and (30), respectively.

In order to achieve the first Equation (29), the combined compensators of negative- and zero-sequence reactive powers must be formed by both a star configuration and a delta configuration of admittances, ($\bar{Y}_A^c, \bar{Y}_B^c, \bar{Y}_C^c$) and ($\bar{Y}_{AB}^c, \bar{Y}_{BC}^c, \bar{Y}_{CA}^c$), connected as Figure 3 represents. The star configuration absorbs opposite reactive currents ($-\bar{I}_{zr}$) and powers ($-\bar{Q}$) as the load, i.e., the admittances ($\bar{Y}_A^c, \bar{Y}_B^c, \bar{Y}_C^c$) are opposite to the load susceptances (Table 5). The delta configuration must absorb the load positive-sequence reactive currents ($\bar{I}_{zr+}$) and powers ($\bar{Q}_+$); therefore, the admittances ($\bar{Y}_{AB}^c, \bar{Y}_{BC}^c, \bar{Y}_{CA}^c$) are opposite to the admittances of the positive-sequence reactive power compensators, indicated in Table 3.

Table 5. Admittances of the combined compensators of negative- and zero-sequence reactive powers.

DELTA CONFIGURATION			STAR CONFIGURATION		
$\bar{Y}_{AB}^c$	$\bar{Y}_{BC}^c$	$\bar{Y}_{CA}^c$	$\bar{Y}_A^c$	$\bar{Y}_B^c$	$\bar{Y}_C^c$
$\frac{1}{3}\bar{B}_+ \dfrac{1}{1-a\bar{\delta}_U}$	$\frac{1}{3}\bar{B}_+ \dfrac{1}{1-\bar{\delta}_U}$	$\frac{1}{3}\bar{B}_+ \dfrac{1}{1-a^2\bar{\delta}_U}$	$-\bar{B}_A$	$-\bar{B}_B$	$-\bar{B}_C$

Therefore, the combined compensators of negative- and zero-sequence reactive powers do not affect the active powers and currents supplied by the source, which have the same values as those absorbed by the load (Table 6). However, these combined compensators supply reactive powers, with values $\bar{Q}_z^c = \bar{Q}_z - \frac{1}{3}\bar{Q}_+$, in each phase ($z = A, B, C$), and, thus, the reactive powers supplied by the source are balanced after the compensation, and their values are reduced (Table 6) up to reach the positive-sequence reactive power absorbed by the load ($\bar{Q}_+$).

Table 6. Active and reactive source powers in systems with combined compensators of negative- and zero-sequence reactive powers ($z = A, B, C$).

ACTIVE	REACTIVE
$\sum_Z P_z = \sum_Z G_z V_{zN}^2$	$\sum_Z (\bar{Q}_z - \bar{Q}_z^c) = \bar{Q}_+$

The connection of combined compensators of negative- and zero-sequence reactive powers, such as Figure 2 represents, reduces the reactive source currents up to reach the values of positive-sequence reactive currents. The active currents are not modified, while the neutral currents are decreased up to the values determined by Equation (21).

3.3.2. Individual Compensators of Negative- and Zero-Sequence Reactive Powers

The individual compensation of negative- and zero-sequence reactive powers is possible using specific compensators, which are able to separately cancel the delivery of these reactive powers from the source. However, the use of these compensators is not recommended for the following reasons:

- the negative-sequence reactive powers are usually negligible compared to the positive-sequence reactive powers, and
- these compensators are hybrid devices, formed by passive elements and electronic converters, which are generally much more expensive than the passive combined compensators for the negative- and zero-sequence reactive powers described in Section 3.3.1.

However, the use of specific compensators of either negative- or zero-sequence reactive powers do not affect the delivery of active source powers since these devices only cancel the negative- and zero-sequence reactive powers, respectively (Table 7).

Table 7. Source active and reactive powers in systems with individual compensators of negative- and zero-sequence reactive powers, ($z = A, B, C$).

	NEGATIVE-SEQUENCE COMPENSATORS	ZERO-SEQUENCE COMPENSATORS
ACTIVE	$\sum_Z P_z = \sum_Z G_z V_{zN}^2$	$\sum_Z P_z = \sum_Z G_z V_{zN}^2$
REACTIVE	$\sum_Z \left(\bar{Q}_z - \frac{1}{3}\bar{Q}_-\right) = \bar{Q}_+ + \bar{Q}_0$	$\sum_Z \left(\bar{Q}_z - \frac{1}{3}\bar{Q}_0\right) = \bar{Q}_+ + \bar{Q}_-$

a)   Individual compensators of negative-sequence reactive powers

These compensators must only absorb negative-sequence reactive powers and currents with opposite values as those absorbed by the load, i.e.:

$$\bar{S}^c = -\bar{Q}_- = -\bar{B}_-^* \cdot V_{AN-}^2 \quad \bar{I}_z^c = -\bar{I}_{zr-} = -\bar{B}_- \bar{V}_{zN-} \quad z = (A, B, C), \quad (30)$$

where $\bar{B}_-$ is the negative susceptance determined as the imaginary part of second Equation (4).

The individual compensators of negative-sequence reactive power are constituted by three admittances $(\bar{Y}_{AB}^c, \bar{Y}_{BC}^c, \bar{Y}_{CA}^c)$ configured in delta (Table 8), which are determined under the consideration that they must absorb the negative-sequence line currents indicated by (30) and, therefore, the currents $(\bar{I}_{ABr-}, \bar{I}_{BCr-}, \bar{I}_{CAr-})$ flowing through each of these admittances must be of negative-sequence, with values as follows:

$$\bar{I}_{ABr-} = \bar{Y}_{AB}^c \cdot \bar{V}_{AB} = -\tfrac{1}{3}\bar{B}_- \cdot \bar{V}_{AB-} \qquad \bar{I}_{BCr-} = \bar{Y}_{BC}^c \cdot \bar{V}_{BC} = -\tfrac{1}{3}\bar{B}_- \cdot \bar{V}_{BC-}$$

$$\bar{I}_{CAr-} = \bar{Y}_{CA}^c \cdot \bar{V}_{CA} = -\tfrac{1}{3}\bar{B}_- \cdot \bar{V}_{CA-} \qquad (31)$$

Table 8. Admittances of the individual compensators of negative-sequence reactive powers

DELTA CONFIGURATION			STAR CONFIGURATION		
$\bar{Y}_{AB}^c$	$\bar{Y}_{BC}^c$	$\bar{Y}_{CA}^c$	$\bar{Y}_A^c$	$\bar{Y}_B^c$	$\bar{Y}_C^c$
$\tfrac{1}{3}\bar{B}_- \dfrac{a\bar{\delta}_U}{1 - a\bar{\delta}_U}$	$\tfrac{1}{3}\bar{B}_- \dfrac{\bar{\delta}_U}{1 - \bar{\delta}_U}$	$\tfrac{1}{3}\bar{B}_- \dfrac{a^2\bar{\delta}_U}{1 - a^2\bar{\delta}_U}$	0	0	0

The connection of specific negative-sequence reactive power compensators only cancels the negative-sequence reactive source currents, but the active and neutral currents remain invariable, with values determined by Equation (1).

b)   Individual compensators of zero-sequence reactive powers

These reactive power compensators have to absorb the following reactive powers and line currents:

$$\bar{S}^c = -\bar{Q}_0 = -\bar{Q} + \bar{Q}_+ + \bar{Q}_- \quad \bar{I}_{rz}^c = -\bar{I}_{zr0} = -\bar{I}_{zr} + \bar{I}_{zr+} + \bar{I}_{zr-} \quad z = (A, B, C), \quad (32)$$

In order to satisfy Equation (32), the individual compensators of zero-sequence reactive powers are constituted by two directly connected configurations, as Figure 3 represents. The star configuration is a total reactive compensator, formed by three admittances $(\bar{Y}_A^c, \bar{Y}_B^c, \bar{Y}_C^c)$, with values indicated in Table 1. The delta configuration is determined by the parallel association of two individual reactive compensators of positive- and negative-sequence, respectively, whose elements have opposite values as those indicated in Tables 3 and 8, respectively (Table 9).

Table 9. Admittances of the zero-sequence reactive power compensators.

DELTA CONFIGURATION			STAR CONFIGURATION		
$\bar{Y}_{AB}^c$	$\bar{Y}_{BC}^c$	$\bar{Y}_{CA}^c$	$\bar{Y}_A^c$	$\bar{Y}_B^c$	$\bar{Y}_C^c$
$\tfrac{1}{3}\dfrac{\bar{B}_+ - a\bar{\delta}_U\bar{B}_-}{1 - a\bar{\delta}_U}$	$\tfrac{1}{3}\dfrac{\bar{B}_+ - \bar{\delta}_U\bar{B}_-}{1 - a\bar{\delta}_U}$	$\tfrac{1}{3}\dfrac{\bar{B}_+ - a^2\bar{\delta}_U\bar{B}_-}{1 - a^2\bar{\delta}_U}$	$-\bar{B}_A$	$-\bar{B}_B$	$-\bar{B}_C$

The connection of individual compensators of zero-sequence reactive powers cancels the zero-sequence reactive source currents as well as reduces the neutral currents up to reach the values determined by Equation (21). The active currents become unmodified after the connection of these compensators.

4. Application Example

The operation of the passive reactive power compensators developed in Section 3 is analyzed in this section with an application example. Likewise, the effectiveness in compensating the reactive power of these devices is compared with that obtained in currently existing passive compensators (such as capacitor banks and Jeon's compensator [20], or similar [21,22]) using the reactive power components as analysis tools. The individual devices to compensate specifically the negative- and zero-sequence reactive powers, described in Section 3.2.2, are not analyzed as they are not passive compensators.

The data used in the application example have been obtained from measurements carried out in the transformation house of a frozen products company. In order to be able to compare with the same criteria, the study of the operation of the aforementioned devices, in terms of reactive power compensation, has been made using only the reactive power supplies recorded to the fundamental frequency. Therefore, the active load powers have not been considered for the analysis since they are not affected by the operation of the capacitor banks, Jeon's compensator as well as the compensators developed in this paper.

The values of voltages, currents and powers summarized in Tables 10, 11 and 12, respectively, have been recorded in the secondary of the transformer of the aforementioned transformation house, using a Fluke 435 Series II analyzer, without having connected any reactive power compensation device. Table 12 also indicates the values calculated for the equivalent reactances of each phase of the load ($\bar{X}_z = \bar{V}_{zN}/\bar{I}_{rz}$,), which are obtained by the quotient between the CRMS values of the line-to-neutral voltages ($\bar{V}_{zN}$, Table 10) and the CRMS values of the reactive currents ($\bar{I}_{rz}$ Table 11) of each phase of the load ($z = A, B, C$).

Table 10. Source voltages.

PHASE	LINE-TO-LINE VOLTAGES		LINE-TO-NEUTRAL VOLTAGES		SYMMETRICAL COMPONENTS		
	VALUE (kVAr)	ANGLE (°)	RMS (V)	ANGLE (°)		RMS (V)	ANGLE (°)
A	387.282	29.96	231.306	0.85	**POSITIVE**	223.79	0
B	387.569	−89.94	216.704	−118.75	**NEGATIVE**	0.24	−83.46
C	387.997	149.98	223.586	117.91	**ZERO**	8.32	26.24

Table 11. Line and neutral currents due to reactive consumptions.

	LINE CURRENTS				SYMMETRICAL COMPONENTS		
	PHASE A	PHASE B	PHASE C	NEUTRAL	POSITIVE	NEGATIVE	ZERO
RMS (A)	291.817	56.729	246.920	228.123	198.422	68.030	76.041
ANGLE (°)	−89.15	151.25	27.91	−40.75	−90.33	−140.00	−40.75

Table 12. Load reactances and power consumptions.

PHASE	EQUIVALENT LOAD REACTANCES		POWER CONSUMPTIONS				
	IMPEDANCE (Ω)	ANGLE (°)	PHASE POWERS		SYMMETRICAL COMPONENTS		
			ACTIVE (W)	REACTIVE (VAR)		ACTIVE (W)	REACTIVE (VAR)
A	0.79264	90	-	67,498.81	**POSITIVE**	−768.78	133,212.2
B	3.82	90	-	12,293.38	**NEGATIVE**	27.00	40.86
C	0.9055	90	-	55,207.91	**ZERO**	741.78	1747.03
TOTAL			-	135,000.1		0	135,000.1

4.1. Compensation of the Total Reactive Power

Three passive devices for fully compensating the reactive power are available. These are the capacitor banks, Jeon's compensator (or equivalent ones) and the TRPC, described in Section 3.1. Values of the reactances of these compensators are indicated in Table 13.

Table 13. Reactances of the total reactive power compensators.

PHASE	CAPACITOR BANK		JEON'S COMPENSATOR		TRPC	
	IMPEDANCE (Ω)	ANGLE (°)	IMPEDANCE (Ω)	ANGLE (°)	IMPEDANCE (Ω)	ANGLE (°)
A	3.3388	−90	0.79264	−90	0.79264	−90
B	3.3388	−90	3.82	−90	3.82	−90
C	3.3388	−90	0.9055	−90	0.9055	−90

Three-phase capacitor banks are built by delta-balanced configurations of capacitors, with the reactances determined as $\bar{X}_c = 9\,V_+^2/\bar{Q}^*$, where V_+ is the RMS value of the positive-sequence line-to-neutral voltages (223.79 V, Table 10) and $\bar{Q}^* = -j135000\,VA$ is the conjugate of the total complex reactive power (Table 12). Jeon's reactive power compensator and the TRPC determined as indicated in Table 1 are constituted by the same elements in this case, in which the active power supplies are not considered. These last two compensators of the total reactive power are formed by three-phase unbalanced star-configured capacitors, with a neutral conductor, whose reactances are indicated in Table 13.

Table 14 reveals that the three types of passive compensators cancel the supply of reactive power from the source. However, the compensation mechanism in capacitor banks is very different as in the other two compensators. Using both Jeon's compensators and TRPC, there are no reactive power components at the source, whereas, with capacitor banks, the source must supply negative and zero sequence reactive powers, which are compensated by absorbing an equal amount of positive-sequence reactive power. The presence of these reactive power components is indicative of an inadequate operation of the capacitor banks, which is confirmed by the non-elimination of the line currents and the maintenance of the value of the neutral current (Table 15), after the connection of capacitors. These currents are necessary for the source to supply the positive-, negative- and zero-sequence powers indicated in Table 14.

Table 14. Active and reactive source powers and their components after compensating.

SYMMETRICAL COMPONENTS	CAPACITOR BANKS		JEON's/TRPC	
	ACTIVE (W)	REACTIVE (VAR)	ACTIVE (W)	REACTIVE (VAR)
POSITIVE	−768.78	−1787.73	0	0
NEGATIVE	27.00	40.70	0	0
ZERO	741.78	1747.03	0	0
TOTAL	0	0	0	0

Table 15. Line and neutral reactive currents after compensating.

COMPENSATOR		LINE CURRENTS				SYMMETRICAL COMPONENTS		
		PHASE A	PHASE B	PHASE C	NEUTRAL	POSITIVE	NEGATIVE	ZERO
CAPACITOR BANKS	RMS (A)	90,793	144.173	46.41	228.123	2.899	67.850	76.041
	ANGLE (°)	−87.12	−30.46	18.64	−40.75	113.27	−139.90	−40.75
JEON's/TRPC	RMS (A)	0	0	0	0	0	0	0
	ANGLE (°)	0	0	0	0	0	0	0

The existence of currents is important for sustainability since energy losses and, therefore, carbon dioxide emissions increase with the square of the RMS values of currents. From Table 15, it can be noted that the connection of Jeon's compensator or the TRPC reduces completely the energy losses and CO2 emissions caused by reactive currents in transformer and lines. However, the connection of capacitor banks decreases the line currents and does not affect the value of the neutral current (Table 15), so the percentage reduction in energy losses and CO2 emissions in the lines and transformer, after connecting delta capacitor banks, are:

$$\Delta W_{p,lines}\% = \left(1 - \frac{90.793^2 + 144.173^2 + 46.41^2 + 228.123^2}{291.817^2 + 56.729^2 + 246.92^2 + 228.123^2}\right) \cdot 100 = 58.675\%$$

$$\Delta W_{p,trafo}\% = \left(1 - \frac{90.793^2 + 144.173^2 + 46.41^2}{291.817^2 + 56.729^2 + 246.92^2}\right) \cdot 100 = 79.12\%$$

4.2. Compensation of the Positive-Sequence Reactive Power

The passive devices for compensating specifically the positive-sequence reactive power (Q_+) are analyzed in this section. These compensators are connected to the transformer secondary, as Figure 5 represents, and they are only constituted by a delta configuration of reactances whose values are calculated according to expressions in Table 3 and summarized in Table 16 (the star connection represented in Figure 3 does not exist for these compensators). These devices are applied to cancel the positive-sequence reactive powers and currents supplied by the sources, as it can be observed in reactive current waveforms represented in Figure 5, in which it can be noted the great reduction in the values of the reactive currents. In addition, current waveforms show the positive-sequence reactive power compensators do not balance the reactive line currents, as was indicated in advance in Section 3.2.

Table 16. Positive-sequence reactive power compensators.

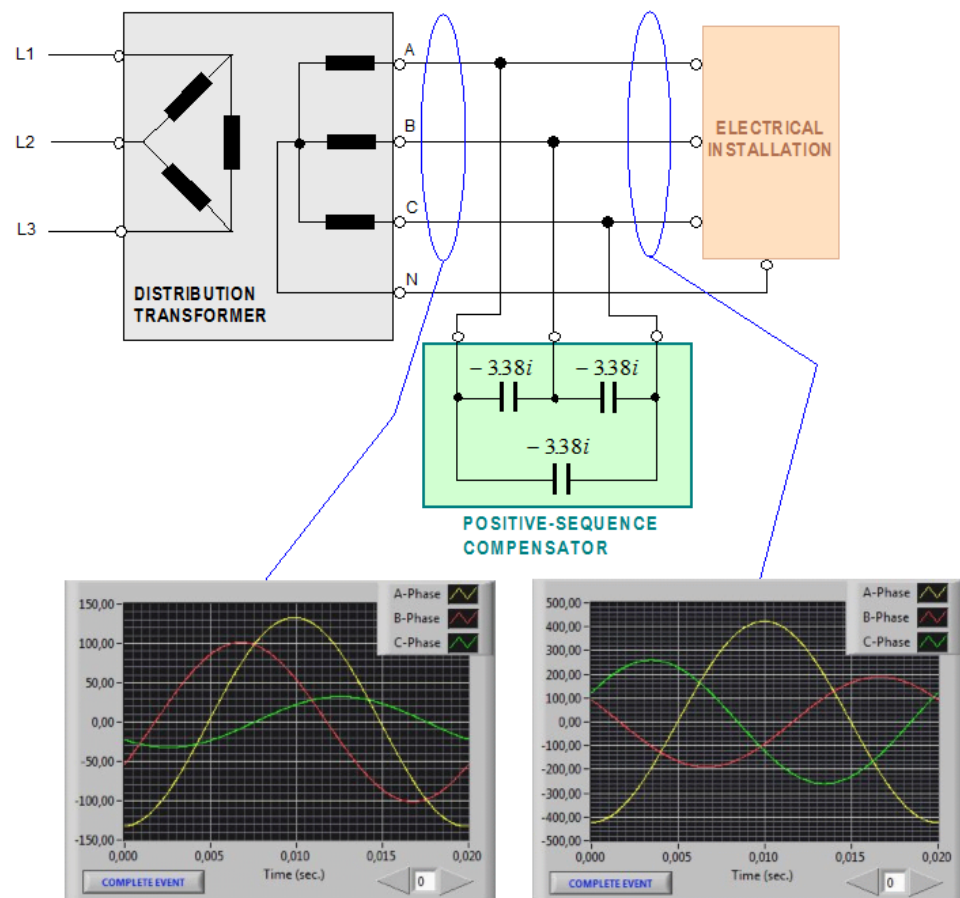| PHASE	$Q_+ -$COMPENSATOR		CAPACITOR BANKS/JEON's COMPENSATOR	
	IMPEDANCE (Ω)	ANGLE (°)	IMPEDANCE (Ω)	ANGLE (°)
AB	3.3807	−90	-	-
BC	3.3832	−90	-	-
CA	3.3869	−90	-	-

Figure 5. Placement of the positive-sequence compensators in the installation, as well as reactive line current waveforms in the transformer secondary and in the electrical installation, obtained representing the Fluke 435 measurements with the LabView platform.

Nowadays, no capacitor banks and Jeon's (or similar) passive compensators are built to compensate only the positive-sequence reactive power separately from the negative- and zero-sequence reactive powers; thus, elements based on technologies of these reactive power compensators cannot be calculated (Table 16).

The impedances of the total positive-sequence reactive power compensators in Table 16 were obtained from the admittance expressions, indicated in Table 3, in which the positive susceptance ($\bar{B}_+$) and the negative-sequence line-to-line unbalanced voltage factor ($\bar{\delta}_U$) are, according to Tables 10 and 11, as follows:

$$\bar{B}_+ = Im\left[\frac{\bar{I}_+}{\bar{V}_{AN+}}\right] = -j0.8866 \ \Omega^{-1} \qquad \bar{\delta}_U = \frac{\bar{V}_{AN-}}{\bar{V}_{AN+}} = 0.0010724\angle 83.46°$$

It is noted in Table 17 the positive-sequence reactive powers supplied by the source are cancelled after the connection of these compensators, which is a significant reduction of the total reactive power, from 135000.1 var up to only 1787.82 var. However, the connection of these compensators creates similar source currents and power losses as the capacitor banks, such as a comparison of Tables 15 and 18 reveals.

Table 17. Active and reactive powers of the source and load and their components after compensating the positive-sequence reactive powers.

SYMMETRICAL COMPONENTS	SOURCE		LOAD	
	ACTIVE (W)	REACTIVE (VAR)	ACTIVE (W)	REACTIVE (VAR)
POSITIVE	−768.78	0	−768.78	133,212.20
NEGATIVE	27.00	40.79	27.00	40.87
ZERO	741.78	1747.03	741.78	1747.03
TOTAL	0	1787.82	0	135,000.1

Table 18. RMS values of the line currents supplied by the source after connecting the positive-sequence reactive power compensator.

	LINE CURRENTS				SYMMETRICAL COMPONENTS		
	PHASE A	PHASE B	PHASE C	NEUTRAL	POSITIVE	NEGATIVE	ZERO
RMS (A)	93.4588	141.61	49.0968	228.123	1.145	67.941	76.041
ANGLE (°)	−87.27	−30.48	19.35	−40.75	179.98	−139.95	−40.75

The percent reduction of energy losses and carbon dioxide emissions in lines and transformers, derived from the connection of the positive-sequence reactive power compensator, are the following:

$$\Delta W_{p,lines}\% = \left(1 - \frac{90.4588^2 + 141.61^2 + 49.0968^2 + 228.123^2}{291.817^2 + 56.729^2 + 246.92^2 + 228.123^2}\right) \cdot 100 = 58.667\%$$

$$\Delta W_{p,trafo}\% = \left(1 - \frac{90.4588^2 + 141.61^2 + 49.0968^2}{291.817^2 + 56.729^2 + 246.92^2}\right) \cdot 100 = 79.11\%$$

Therefore, the sustainability improvement in transformers and lines caused by the connection of positive-sequence compensators is practically the same as this due to the connection of capacitor banks.

4.3. Combined Compensation of the Negative- and Zero-Sequence Reactive Powers

The combined compensators of negative- and zero-sequence reactive powers are connected, as Figure 6 represents. In this application, these devices are formed by a delta configuration of coils, with opposite values as the positive-sequence reactive power compensator (Table 16), directly connected to a star configuration of capacitors, with the same values as the TRPC (Table 13), such as it is summarized in Table 19. These compensators are used for balancing the reactive source power deliveries, as noted in the waveforms of the transformer secondary reactive currents (Figure 6).

Table 19. Combined compensators of negative- and zero-sequence reactive powers.

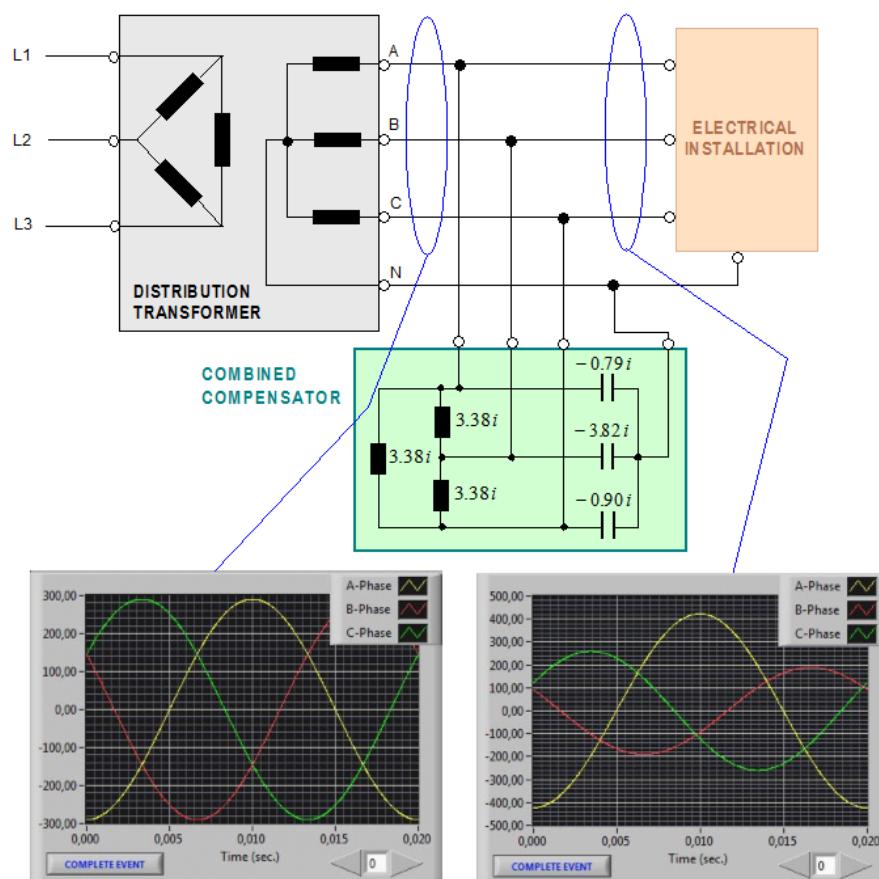| PHASE	COMBINED COMPENSATOR				CAPACITOR BANKS/JEON's COMPENSATOR	
	DELTA CONFIGURATION		STAR CONFIGURATION			
	IMPEDANCE (Ω)	ANGLE (°)	IMPEDANCE (Ω)	ANGLE (°)	IMPEDANCE (Ω)	ANGLE (°)
AB (A)	3.3807	90	0.79264	−90	-	-
BC (B)	3.3832	90	3.82	−90	-	-
CA (C)	3.3869	90	0.9055	−90	-	-

Figure 6. Placement of the combined compensators in the installation, as well as reactive line current waveforms in the transformer secondary and in the electrical installation, obtained representing the Fluke 435 measurements with the LabView platform.

Today, there are no capacitor banks and Jeon's (or similar) passive compensators that can compensate both the negative- and zero-sequence reactive powers separately from the positive-sequence reactive power (Table 19).

It is noted in Tables 20 and 21 that the negative- and zero-sequence reactive source powers and currents have been cancelled after connecting the combined compensator indicated in Table 19. Thus, the reactive supplies of source powers and currents have been balanced, with only positive-sequence components. This implies the sustainability of this installation has been improved.

Table 20. Source and load of active and reactive powers and their components after compensating together the negative- and zero-sequence reactive powers.

SYMMETRICAL COMPONENTS	SOURCE		LOAD	
	ACTIVE (W)	REACTIVE (VAR)	ACTIVE (W)	REACTIVE (VAR)
POSITIVE	0	133,212.20	−768.78	133,212.20
NEGATIVE	0	0	27.00	40.87
ZERO	0	0	741.78	1747.03
TOTAL	0	133,212.20	0	135,000.1

Table 21. RMS line currents supplied by the source after connecting the combined compensator of negative- and zero-sequence reactive powers.

	LINE CURRENTS				SYMMETRICAL COMPONENTS		
	PHASE A	PHASE B	PHASE C	NEUTRAL	POSITIVE	NEGATIVE	ZERO
RMS (A)	198.419	198.419	198.419	0	198.419	0	0
ANGLE (°)	−90	150	30	24.78	−90	−173.27	24.78

The percent reduction of energy losses and carbon dioxide emissions in lines and transformers are the following, after connecting these combined compensators:

$$\Delta W_{p,lines}\% = \left(1 - \frac{3 \cdot 198.419^2}{291.817^2 + 56.729^2 + 246.92^2 + 228.123^2}\right) \cdot 100 = 41.35\%$$

$$\Delta W_{p,trafo}\% = \left(1 - \frac{3 \cdot 198.419^2}{291.817^2 + 56.729^2 + 246.92^2}\right) \cdot 100 = 20.914\%$$

The reductions derived from the operation of these compensators are lower than in the previous ones because the negative- and zero-sequence reactive powers are much less important in power systems.

5. Conclusions

Several devices for compensating the positive-, negative-, and zero-sequence components of the reactive power in three-phase, four-wire sinusoidal systems, supplied with unbalanced voltages, have been developed in this paper, for the first time in the technical literature. Some of these compensators are passive, formed by reactances (Figures 1a and 1b), while others are hybrid, formed by passive elements and electronic converters (Figures 1c and 1d). Within the latter are the negative- and zero-sequence individual reactive power compensators. Likewise, passive devices for the total reactive power compensation (TRPC) have been established in this paper.

The comparison between the passive reactive power compensation devices developed in this paper and the passive reactive power compensators known today, such as capacitor banks and Jeon's compensators [19], when the supply voltages are unbalanced, determined that:

- The capacitor banks and Jeon's compensators are able to fully compensate the reactive power; however, they cannot compensate the positive-sequence reactive component and the combined negative- and zero-sequence reactive components separately from the total reactive power.
- TRCP and Jeon's compensators allow achieving 100% reductions in source energy losses and carbon dioxide emissions caused by the circulation of reactive currents, in all distribution networks, with independence of the system unbalance degrees. However, reductions obtained with capacitor banks are less, between 60% and 80% in most analyzed distribution networks, depending on the voltage and load unbalance degrees. These lower performances of the capacitor banks are justified by the compensation mechanism of these devices, in which the cancellation of the reactive source power does not eradicate the presence of positive-, negative-, and zero-sequence powers at the source when voltages are unbalanced.
- The individual compensators for the positive-sequence reactive powers achieve reductions of source energy losses and carbon dioxide emissions in a similar amount as the traditional capacitor banks, between 60% and 80% in most analyzed distribution networks, depending on the imbalances.
- The combined compensator of negative- and zero-sequence reactive powers are able to cancel the circulation of reactive currents through the neutral conductor; therefore, these compensators are more effective in the reduction of power losses in the neutral

wire than the traditional capacitor banks. However, the reductions in source energy losses and carbon dioxide emissions of the combined compensators of negative- and zero-sequence reactive powers are usually modest, only 20% to 40% in most analyzed distribution networks, especially due to the small values that the negative-sequence reactive powers have in power systems, as a consequence of the negative-sequence voltage limitations, imposed by different standards.

Although combined- and positive-sequence reactive power compensators do not improve facilities' sustainability as much as TRPCs, these passive devices are also useful in other applications where positive sequence reactive power needs to be compensated or maintained. These applications will be the object of study in future works.

Institutional Review Board Statement: Not applicable.

Informed Consent Statement: Not applicable.

Data Availability Statement: Not applicable.

Conflicts of Interest: The authors declare no conflicts of interest. The funders had no role in the design of the study; in the collection, analyses, or interpretation of data; in the writing of the manuscript; or in the decision to publish the results.

References

1. Stanley, W., Jr. Phenomena of Retardation in the Induction Coil. *Am. Inst. Electr. Eng.* **1888**, *V*, 97–115.
2. Shallenberger, O.B. The distribution of Electricity by Alternative Current. *Electrical World*. **1888**, *1*, 114–115.
3. Steinmetz, C.P. *Theory of Alternating Current Phenomena*; McGraw: New York, NY, USA, 1897.
4. Lyon, W.V. Reactive Power and Power Factor. In Proceedings of the North Eastern District Meeting of the AIEE, Schenectady, New York, NY, USA, 10–12 May 1933.
5. Budeanu, C.I. *Puissances reactives et fictives*; Institut Romain De L'energie: Bucharest, Romania, 1927.
6. Curtis, H.L.; Silsbee, F.B. Definitions of Power and Related Quantities. *Electr. Eng.* **1935**, *54*, 394–404.
7. Emanuel, A.E. Powers in nonsinusoidal situations a review of definitions and physical meaning. *IEEE Trans. Power Deliv.* **1990**, *5*, 1377–1389.
8. Jeon, S.-J. Considerations on a Reactive Power Concept in a Multiline System. *IEEE Trans. Power Deliv.* **2006**, *21*, 551–559.
9. Czarnecki, L.S. Physical Interpretation of the Reactive Power in Terms of the CPC Power Theory. *Electr. Power Qual. Util. J.* **2007**, *XIII*, 89–95.
10. IEEE Standard 1459 2010. *IEEE Trial Use Standard for the Measurement of Electric Power Quantities under Sinusoidal, Non-sinusoidal, Balanced or Unbalanced Conditions*; IEEE Power and Energy Society: New York, NY, USA, 2010.
11. Fortescue, C.L. Method of symmetrical coordinates applied to solution of poly-phase networks. In Proceedings of the 34th Convention of American Institute of Electrical Engineers, Atlantic City, NJ, USA, 28 June 1918; https://doi.org/10.1109/T-AIEE.1918.4765570.
12. Fortescue, C.L. Power, Reactive Volt-Amperes, Power Factor. *Transactions of the American Institute of Electrical Engineers*. **1933**, *52*(3), 758-762, doi: 10.1109/T-AIEE.1933.5056392.
13. National Electrical Manufacturers Association (NEMA). Publication No. MG1-1998: Motors and Generators. Available online: https://www.nema.org/standards/view/motors-and-generators (accessed on 1 October 2021)
14. Driesen, J.; Van Craenenbroeck, T. Voltage Disturbances: Introduction to Unbalance. *Power Quality Application Guide, Copper Development Association*. **2002**, *5*, 3.
15. European Standard EN 50160. Voltage Characterisitics of Electricity Supplied by Public Distribution Systems. Available online: https://orgalim.eu/position-papers/en-50160-voltage-characteristics-electricity-supplied-public-distribution-system (accessed on 1 October 2021)

16. *Voltage Unbalance and Motors*; Pacific Gas and Electric Company: October 2009. Available online: https://www.pge.com/includes/docs/pdfs/mybusiness/customerservice/energystatus/powerquality/voltage_unbalance_rev2.pdf (accessed on 1 October 2021)

17. Ghassemi, F.; Perry, M. Review of Voltage Unbalance Limits in the GB Grid Code CC.6.1.5.(b). Available online: https://www.nationalgrid.com/sites/default/files/documents/37643-Voltage%20Unbalance%20Report.pdf (Accessed on 1 October 2021)

18. ANSI 84.1-2020. American National Standard for Electric Power Systems and Equipment—Voltage Ratings (60 Hz). Available online: https://www.nema.org/standards/view/American-National-Standard-for-Electric-Power-Systems-and-Equipment-Voltage-Ratings (Accessed on 1 October 2021)

19. León Martínez, V.; Montañana-Romeu, J.; Roger-Folch, J.; Navarro, A.C. Why reactive compensators do not improve the efficiency correctly in unbalanced circuits. In *XIX IMEKO World Congress Fundamental and Applied Metrology*, September 6–11, 2009, IMEKO: Lisbon, Portugal. ISBN 978-963-88410-0-1.

20. Jeon, S.-J.; Willems, J.L. Reactive power compensation in a multi-line system under sinusoidal unbalanced conditions. *Int. J. Circuit Theory Appl.* **2010**, *39*, 211–224, https://doi.org/10.1002/cta.629.

21. Blasco, P.A.; Montoya-Mira, R.; Díez, J.M.; Montoya, R.; Reig, M.J. Compensation of Reactive Power and Unbalanced Power in Three-Phase Three-Wire Systems Connected to an Infinite Power Network. *Appl. Sci.* **2020**, *10*, 113, https://doi.org/10.3390/app10010113.

22. Montoya-Mira, R.; Blasco, P.A.; Díez, J.M.; Montoya, R.; Reig, M.J. Unbalanced and Reactive Currents Compensation in Three-Phase Four Wire Sinusoidal Power Systems. *Appl. Sci.* **2020**, *10*, 1764, https://doi.org/10.3390/app10051764.

23. Akagi, H.; Kanazawa, Y.; Nabae, A. Instantaneous reactive power compensators comprising switching devices without energy storage components. *IEEE Trans. Ind. Appl.* **1984**, *20*, 625–630, https://doi.org/10.1109/TIA.1984.4504460.

24. Emanuel, A.E.; Chakravorti, A.K. A current regulated switched capacitor static volt ampere reactive compensator. *IEEE Trans. Ind. Appl.* **1994**, *30*, 986–997. https://doi.org/10.1109/28.297916.

25. Czarnecki, L.S.; Hsu, S.M.; Chen, G. Adaptive balancing compensator. *IEEE Trans. Power Deliv.* **1995**, *10*, 1663–1669, https://doi.org/10.1109/61.400954.

26. Devaraju, T.; Reddy, V.C.V.; Kumar, M.V. Role of custom power devices in Power Quality Enhancement: A Review. *Int. J. Eng. Sci. Technology.* **2010**, *2*, 3628–3634.

27. Dixon, J.; Moran, L.; Rodriguez, J.; Domke, R. Reactive Power Compensation Technologies: State-of-the-Art Review. *Proc. IEEE*, **2005**, *93*, 2144–2164, https://doi.org/10.1109/JPROC.2005.859937.

28. Quintela, F.R.; Arévalo, J.M.G.; Redondo, R.C. Power analysis of static VAr compensators. *Int. J. Electr. Power Energy Syst.* **2008**, *30*, 376–382, https://doi.org/10.1016/j.ijepes.2007.12.002.

29. Ambriz-Perez, H.; Acha, E.; Fuerte-Esquivel, C.R. Advanced SVC models for Newton-Raphson load flow and Newton optimal power flow studies. *IEEE Trans. Power Syst.* **2000**, *15*, 129–136, https://doi.org/10.1109/59.852111.

30. Rao, B.V.; Kumar, G.V.N.; Priya, M.R.; Sobhan, P.V.S. Implementation of Static VAR Compensator for Improvement of Power System Stability. In *2009 International Conference on Advances in Computing, Control, and Telecommunication Technologies*; 2009; pp. 453–457. https://doi.org/10.1109/ACT.2009.117.

31. Said, I.K.; Pirouti, M. Neural network-based load balancing and reactive power control by Static VAR compensator. *Int. J. Comput. Electr. Eng.* **2009**, *1*, 25–31.

32. Xu, L.; Yao, L.; Sasse, C. Comparison of using SVC and STATCOM for wind farm integration. In Proceedings of the IEEE 2006 International Conference on Power System Technology, Chongqing, China, 22–26 October 2006; pp 1–7. https://doi.org/ICPST.2006.321663.

33. STATCOM Replaces Critical Urban Generation for Voltage Control and Stability; ABB: Västerås, Sweden, 2011. Available online: https://library.e.abb.com/public/525e8cf8cebf2597c1257878004023e7/A02-0200%20E%20LR.pdf (accessed on 1 October 2021).

34. A Matter of Facts. Deliver More, High Quality Power. ABB: Västerås, Sweden, 2016. Available online: https://search.abb.com/library/Download.aspx?DocumentID=1JNS018770&LanguageCode=en&DocumentPartId=&Action=Launch (accessed on 1 October 2021).

35. Parallel Compensation. Comprehensive Solutions for Safe and Reliable Grid Operation. Siemens AG Erlangen, Germany, 2016. Available on: https://pdf.directindustry.com/pdf/siemens-high-voltage-power-transmission/parallel-compensation-comprehensive-solutions-safe-reliable-grid-operation/32878-889649.html (accessed on 1 October 2021)

36. Neyshabouri, Y.; Chaudhary, S.K.; Teodorescu, R.; Sajadi, R.; Iman-Eini, H. Improving the Reactive Current Compensation Capability of Cascaded H-Bridge Based STATCOM Under Unbalanced Grid Voltage. *IEEE J. Emerg. Sel. Top. Power Electron.* **2020**, *8*, 1466–1476, https://doi.org/10.1109/JESTPE.2019.2916571.

37. Tamboli, A.S.; Jadhav, H.T. Hybrid STATCOM for Reactive Power Compensation. In Proceedings of the 2018 International Conference on Current Trends towards Converging Technologies (ICCTCT), Coimbatore, India, 1–3 March 2018; pp. 1–5. https://doi.org/10.1109/ICCTCT.2018.8550889.

38. Kumar, C.; Mishra, M.K. An Improved Hybrid DSTATCOM Topology to Compensate Reactive and Nonlinear Loads. *IEEE Trans. Ind. Electron.* **2014**, *61*, 6517–6527, https://doi.org/10.1109/TIE.2014.2321355.